# Self-averaging behavior at the metal-insulator transition of many-body quantum systems out of equilibrium

E. Jonathan Torres-Herrera,[1] Mauro Schiulaz,[2] Francisco Pérez-Bernal,[3] and Lea F. Santos[2]

[1]*Instituto de Física, Benemérita Universidad Autónoma de Puebla, Apt. Postal J-48, Puebla, 72570, Mexico*
[2]*Department of Physics, Yeshiva University, New York City, New York, 10016, USA*
[3]*Dep. CC. Integradas y Centro de Estudios Avanzados en Física,*
*Matemáticas y Computación. Fac. CC. Experimentales, Universidad de Huelva, Huelva 21071,*
*& Instituto Carlos I de Física Teórica y Computacional, Universidad de Granada, Granada 18071, Spain*
(Dated: October 25, 2019)

An observable of a disordered system is self-averaging when its properties do not depend on the specific realization considered. Lack of self-averaging, on the other hand, implies that sample to sample fluctuations persist no matter how large the system is. The latter scenario is often found in the vicinity of critical points, such as at the metal-insulator transition of interacting many-body quantum systems. Much attention has been devoted to these systems at equilibrium, but little is known about their self-averaging behavior out of equilibrium, which is the subject of this work. We consider two local and two non-local quantities in real space that are of great experimental and theoretical interest. In the metallic phase, we show that their self-averaging behavior is highly dependent on the observable itself and on the time scale, but the picture simplifies substantially as we approach localization. In this phase, the local quantities are self-averaging at any time, while the non-local ones are non-self-averaging at all time scales.

## I. INTRODUCTION

When dealing with disordered systems, a central question is whether self-averaging holds or not [1]. A quantity is self-averaging when the ratio between its variance over disorder realizations and the square of its average decreases with system size [2–10]. This implies that the number of samples used in experiments and statistical analyses can be reduced as the system size increases. It also means that in the thermodynamic limit, the quantity's behavior does not depend on any particular disorder realization. If self-averaging does not hold, averages over large sets of realizations are needed no matter how large the system is.

Studies of self-averaging are commonly associated with the analyses of normal and anomalous diffusion [11–14] and with transitions into the spin-glass state [5, 15, 16]. A variety of quantities have been investigated, from susceptibility, specific heat, and conductance to order parameter, free energy, and entanglement entropy. At critical points, self-averaging is usually absent [2–9, 17–19].

In recent numerical studies of interacting many-body quantum systems with onsite disorder, self-averaging is often assumed to hold in the chaotic regime, while more care is taken only in the vicinity of the metal-insulator transition. For this case, discussions about the violation of self-averaging have been made mostly in the context of systems at equilibrium [20–22]. Very few works target the self-averaging properties of these many-body quantum systems out of equilibrium, with the existing ones concentrating on driven systems [10, 23] or on the two-level form factor [24–28], which is simply an alternative to analyze spectral properties in the time domain.

When we first approached the subject of self-averaging, our original goal was to fill this gap by analyzing what happens to the self-averaging behavior of interacting quantum systems out of equilibrium. The plan was to investigate how the behavior of different quantities and at different time scales would change as the disorder strength increases and the system approaches a many-body localized phase. To our surprise, we found analytically and confirmed numerically that even in the chaotic regime, when the disorder strength is of the order of the coupling parameters, some quantities are non-self-averaging, the results depending strongly on the quantity and on the time scale. The paper that we ended up writing was then entirely dedicated to the chaotic regime [29]. In this new work, we come back to our original goal and investigate the self-averaging properties of an interacting spin model out of equilibrium as a function of its disorder strength.

We consider four quantities that have been extensively studied in nonequilibrium quantum dynamics: survival probability, inverse participation ratio, spin autocorrelation function, and connected spin-spin correlation function. The first two are non-local in space and the last two are local quantities studied experimentally. The spin autocorrelation function is equivalent to the density imbalance used in experiments with cold atoms [30] and the connected spin-spin correlation function is measured in experiments with ion traps [31].

In the chaotic regime, the results are non-trivial. The survival probability is not self-averaging at any time scale, the inverse participation ratio is self-averaging only at long times, the spin autocorrelation function is self-averaging only at short times, and the connected spin-spin correlation function is self-averaging at any time scale [29]. At localization, we show that the results become rather simple: our local quantities are self-averaging at any time scale and our non-local quantities are non-self-averaging at all times. We also provide several numerical results and justifications for the vari-

ous behaviors encountered as the system moves from the metallic to the insulating phase.

The paper is organized as follows. Self-averaging is defined in Sec. II, where we present also the model, initial states, and observables. Each one of the next four sections is then dedicated to one of the four quantities investigated. The plots contain on the left columns the entire evolution of the average values of the observables and on the right columns, the corresponding results for the relative variances. Conclusions are given in Sec. VII.

## II. SELF-AVERAGING, MODEL, INITIAL STATES, AND OBSERVABLES

This section defines the property of self-averaging and presents the spin model, the picked initial states and the quantities that we study.

### A. Self-Averaging

A quantity $O$ is self-averaging when its relative variance, that is the ratio between its variance $\sigma_O^2$ over disorder realizations and the square of its mean,

$$\mathcal{R}_O(t) = \frac{\sigma_O^2(t)}{\langle O(t)\rangle^2} = \frac{\langle O^2(t)\rangle - \langle O(t)\rangle^2}{\langle O(t)\rangle^2}, \qquad (1)$$

goes to zero as the system size $L$ increases. The notation $\langle . \rangle$ in the equation above indicates average over disorder realizations. In our case, it also includes averages over initial states. These states are all very similar, as we stress later, since we take them in a very narrow window of energy around the center of the spectrum. The decrease of the relative variance with $L$ implies that in the thermodynamic limit, the sample to sample fluctuations vanish.

Strong self-averaging refers to the case where $\mathcal{R}_O(t) \sim L^{-1}$, and weak self-averaging means that $\mathcal{R}_O(t) \sim L^{-\nu}$ with $0 < \nu < 1$. In many-body quantum systems, where the initial state can eventually spread over an exponentially large many-body Hilbert space, one can also encounter what we call "super" self-averaging, when the relative variance decreases exponentially with the system size [29].

We emphasize that self-averaging is a concept intrinsically related with the presence of randomness in the system. The relative variance, $\mathcal{R}_O(t)$, that we study here involves averages over disorder realizations. It is different from relative variances involving temporal averages,

$$\mathcal{T}_O = \frac{\overline{O^2} - \overline{O}^2}{\overline{O}^2}, \qquad (2)$$

where

$$\overline{O} = \lim_{T \to \infty} \frac{1}{T} \int_0^T O(t)dt. \qquad (3)$$

While $\mathcal{R}_O(t)$ depends on time, $\mathcal{T}_O$ is time independent. $\mathcal{T}_O$ is employed in studies of equilibration and thermalization [32–35].

Equilibration happens after the relaxation time $t_R$, when the dynamics finally saturates and the observable simply fluctuates around its infinite time average $\overline{O}$. At this large time scales one can expect $\mathcal{R}_O(t > t_R)$ to coincide with $\mathcal{T}_O$ when the system is chaotic, since ergodicity implies that time averages and ensemble averages agree.

### B. Model and Initial State

We consider a one-dimensional spin-$1/2$ model with local two-body interactions and onsite static disorder. The Hamiltonian is given by

$$H = H_{\mathrm{h}} + H_{\mathrm{XXZ}}, \qquad (4)$$

where

$$H_{\mathrm{h}} = J\sum_{k=1}^{L} h_k S_k^z,$$

$$H_{\mathrm{XXZ}} = J\sum_{k=1}^{L}(S_k^x S_{k+1}^x + S_k^y S_{k+1}^y + S_k^z S_{k+1}^z). \qquad (5)$$

Above, $\hbar = 1$, $S_k^{x,y,z}$ are the spin operators on site $k$, $L$ is the size of the chain, which has periodic conditions, and $J$ sets the energy scale. The Zeeman splitting on each site is $Jh_k$, where $h_k$ are independent random numbers uniformly distributed in $[-h, h]$ and $h$ is the disorder strength. The total magnetization in the $z$-direction is conserved. We work in the largest subspace, which has zero total $z$-magnetization and dimension $D = L!/(L/2)!^2$.

The model is integrable when $h = 0$. It becomes chaotic when $h \sim 1$, due to the interplay between disorder and the Ising interaction $S_k^z S_{k+1}^z$. It approaches a many-body localized phase when the disorder strength is larger than a critical value, $h > h_c$ [36–40].

We denote the eigenstates of $H_{\mathrm{h}}$ by $|n\rangle$ and the eigenstates and eigenvalues of $H$ by $|\alpha\rangle$ and $E_\alpha$, respectively. The initial state $|\Psi(0)\rangle$ that we choose is an eigenstate of $H_{\mathrm{h}}$ with energy very close to the center of the spectrum,

$$E_0 = \langle\Psi(0)|H|\Psi(0)\rangle = \sum_\alpha \left|c_\alpha^0\right|^2 E_\alpha \sim 0, \qquad (6)$$

where $c_\alpha^0 = \langle\alpha|\Psi(0)\rangle$.

For each curve in the plots of this work, we perform averages over $0.01D$ initial states with $E_0 \sim 0$ and $10^4/(0.01D)$ disorder realizations, so that the total amount of data is $\sim 10^4$.

### C.  Quantities

We investigate the self-averaging behavior of two non-local quantities in space, the survival probability and the inverse participation ratio, and two local experimental observables, the spin autocorrelation function and the connected spin-spin correlation function.

#### 1.  Survival Probability

The survival probability gives the probability to find the initial state later in time [41–56],

$$P_S(t) = \left| \langle \Psi(0)| e^{-iHt} |\Psi(0)\rangle \right|^2 = \left| \sum_\alpha \left| c_\alpha^0 \right|^2 e^{-iE_\alpha t} \right|^2. \tag{7}$$

It is a non-local quantity in space and also in time, since it is an autocorrelation function. It can be written in an integral form as

$$P_S(t) = \left| \int \rho_0(E) e^{-iEt} dt \right|^2, \tag{8}$$

where

$$\rho_0(E) = \sum_\alpha \left| c_\alpha^0 \right|^2 \delta(E - E_\alpha) \tag{9}$$

is the energy distribution of the initial state. The square of the width of $\rho_0(E)$,

$$\Gamma^2 = \sum_{n\neq 0} |\langle n|H|\Psi(0)\rangle|^2, \tag{10}$$

is related to the number of states $|n\rangle$ directly coupled to the initial state, which is $\propto L$ for our spin model.

#### 2.  Inverse Participation Ratio

The inverse participation ratio quantifies the spread of the initial state in the many-body Hilbert space defined by the states $|n\rangle$ [57]. It can be written as an out-of-time order correlator where the operators are projection operators [58]. It is given by

$$\text{IPR}(t) = \sum_n \left| \langle n| e^{-iHt} |\Psi(0)\rangle \right|^4. \tag{11}$$

At $t = 0$, $\text{IPR}(0) = 1$. At short times, the initial decaying behavior is very similar to the square of the survival probability. This changes as $|\Psi(0)\rangle$ spreads and the dynamics pick up the other states $|n\rangle$.

#### 3.  Spin Autocorrelation Function

The spin autocorrelation function measures how close the spin configuration in the $z$-direction at a time $t$ is to the initial spin configuration,

$$I(t) = \frac{4}{L} \sum_{k=1}^L \langle \Psi(0)| S_k^z e^{iHt} S_k^z e^{-iHt} |\Psi(0)\rangle. \tag{12}$$

This quantity is similar to the density imbalance between even and odd sites measured in experiments with cold atoms [30].

#### 4.  Connected Spin-Spin Correlation Function

The connected spin-spin correlation function is given by

$$C(t) = \frac{4}{L} \sum_k \left[ \langle \Psi(t)| S_k^z S_{k+1}^z |\Psi(t)\rangle \right. \tag{13}$$
$$\left. - \langle \Psi(t)| S_k^z |\Psi(t)\rangle \langle \Psi(t)| S_{k+1}^z |\Psi(t)\rangle \right].$$

It is measured in experiments with ion traps [31].

## III.  SURVIVAL PROBABILITY

In the chaotic regime, the survival probability is not self-averaging at any time scale [29]. This was shown analytically by evolving $P_S(t)$ with full random matrices. Based on numerical results for all times and analytical results for short and long times, we verified that the same is true also for the disordered chaotic spin model [29]. As we now explain, the survival probability remains non-self-averaging at all times as the disorder strength increases and the system approaches localization.

### A.  Short Times: $\mathbf{t < \Gamma^{-1}}$

An expansion for short times gives $\mathcal{R}_{P_S}(t < \Gamma^{-1}) = \sigma_{\Gamma^2}^2 t^4 + \mathcal{O}(t^6)$, where $\sigma_{\Gamma^2}^2 = \langle \Gamma^4 \rangle - \langle \Gamma^2 \rangle^2$. This result is independent of the disorder strength. According to Eq. (10), $\Gamma^2$ only depends on the off-diagonal elements of $H$, while the disorder enters on the diagonal elements. This implies that the relative variance of $P_S$ increases linearly with system size for any (reasonable value of the) disorder strength,

$$\mathcal{R}_{P_S}(t < \Gamma^{-1}) \propto J^4 t^4 L, \tag{14}$$

This is indeed what we see in Fig. 1, where we show the average value of the survival probability on the left panels and its relative variance on the right panels for six values of the disorder strength, from top panel to bottom panel: $h = 0.75, 1, 1.5, 2, 3, 4$. The value $h = 0.75$ represents the chaotic region and for $h = 4$, the system should already

be in the localized phase. There is not much difference in the behavior of $\mathcal{R}_{P_S}(t)$ at short times for the different disorder strengths.
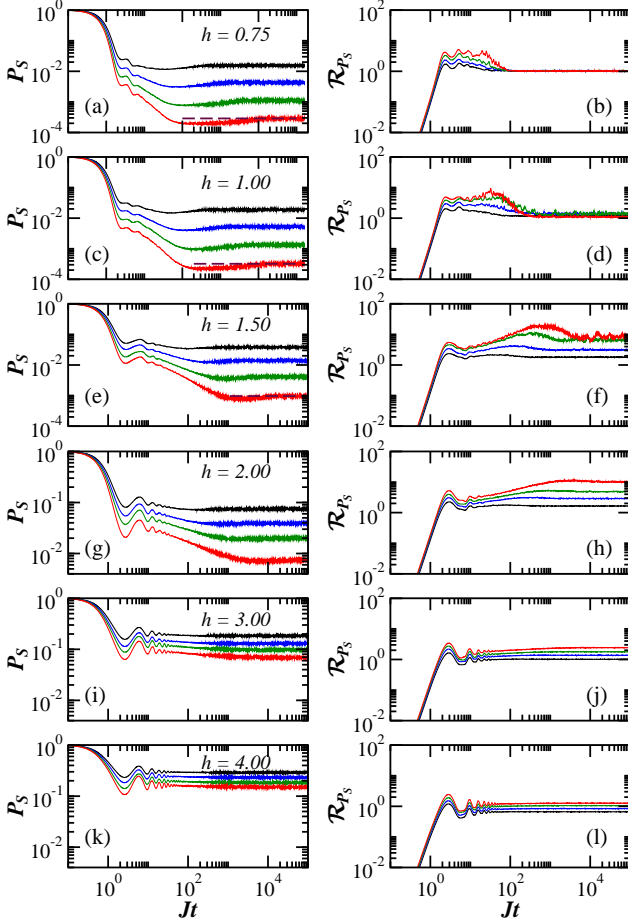


FIG. 1. Left panels: Mean value of the survival probability. Right panels: Relative variance of the survival probability. The values of the disorder strength are indicated on the left panels, they increase from the top to the bottom panel. The curves correspond to system sizes $L = 10$ (black), 12 (blue), 14 (green), and 16 (red). On each left panel, $L$ increases from top to bottom and the horizontal dashed line for $L = 16$ indicates the saturation point.

### B. Long Times: $t > t_R$

At times beyond the saturation of the dynamics, that is for $t > t_R$, the survival probability for each disorder realization fluctuates around its infinite-time average,

$$\overline{P_S} = \sum_\alpha \left|c_\alpha^0\right|^4. \tag{15}$$

This is because in the absence of too many degeneracies in the spectrum, the first term on the right hand side of

the equation

$$\overline{P_S(t)} = \overline{\sum_{\alpha \neq \beta} |c_\alpha^0|^2 |c_\beta^0|^2 e^{-i(E_\alpha - E_\beta)t}} + \sum_\alpha \left|c_\alpha^0\right|^4$$

cancels out. Equivalently, for the disorder average of the survival probability at long times, the first term on the right hand side of the equation

$$\langle P_S(t > t_R) \rangle = \left\langle \sum_{\alpha \neq \beta} |c_\alpha^0|^2 |c_\beta^0|^2 e^{-i(E_\alpha - E_\beta)t} \right\rangle + \left\langle \sum_\alpha \left|c_\alpha^0\right|^4 \right\rangle$$

also cancels out, so

$$\langle P_S(t > t_R) \rangle = \left\langle \sum_\alpha \left|c_\alpha^0\right|^4 \right\rangle. \tag{16}$$

To compute $\mathcal{R}_{P_S}(t > t_R)$, we need

$$\langle P_S^2(t > t_R) \rangle =$$
$$\left\langle \sum_{\alpha,\beta,\gamma,\delta} |c_\alpha^0|^2 |c_\beta^0|^2 |c_\gamma^0|^2 |c_\delta^0|^2 e^{-i(E_\alpha - E_\beta + E_\gamma - E_\delta)t} \right\rangle.$$

In the equation above, the terms that do not average out are $\alpha = \beta, \gamma = \delta, \alpha \neq \delta$, and $\alpha = \delta, \beta = \gamma, \alpha \neq \beta$, and $\alpha = \beta = \gamma = \delta$. Therefore,

$$\langle P_S^2(t > t_R) \rangle = 2 \left\langle \sum_{\alpha \neq \beta} \left|c_\alpha^0\right|^4 \left|c_\beta^0\right|^4 \right\rangle + \left\langle \sum_\alpha \left|c_\alpha^0\right|^8 \right\rangle.$$

and

$$\mathcal{R}_{P_S}(t > t_R) = \tag{17}$$
$$\frac{2 \left\langle \left(\sum_\alpha |c_\alpha^0|^4\right)^2 \right\rangle - \left\langle \sum_\alpha |c_\alpha^0|^4 \right\rangle^2 - \left\langle \sum_\alpha |c_\alpha^0|^8 \right\rangle}{\left\langle \sum_\alpha |c_\alpha^0|^4 \right\rangle^2}.$$

In the chaotic regime, the eigenstates away from the edges of the spectrum and therefore also the initial states are similar to the eigenstates from full random matrices, that is, they are approximately normalized random vectors. This means that the coefficients $c_\alpha^0$ are approximately random numbers from a Gaussian distribution with the constraint $\sum_\alpha \left|c_\alpha^0\right|^2 = 1$. In this case,

$$\langle P_S(t > t_R) \rangle = \langle \overline{P_S} \rangle \propto \frac{1}{D} \tag{18}$$

and

$$\mathcal{R}_{P_S}(t > t_R) \simeq 1, \tag{19}$$

which implies that the long-time relative variance of the survival probability in the chaotic regime is independent of the system size. The lack of self-averaging in this case is connected with the remaining memory of the initial state, which is a characteristic of autocorrelation functions.

As the disorder strength increases above 1, the eigenstates of the system get further away from those of full random matrices, correlations build up between their components and the fluctuations of $P_S(t)$ at long times increase. In this case, $\mathcal{R}_{P_S}(t > t_{\mathrm{R}})$ becomes dependent on $L$ and reaches values even larger than 1, as seen on the right panels of Fig. 1. For a given system size, the largest values of $\mathcal{R}_{P_S}(t > t_{\mathrm{R}})$ appear in the intermediate region between chaos and localization, with the case of $h = 2$ in Fig. 1 (h) serving as a good example. This is the region where the eigenstates become fractal [59–62], so that they are very different from each other even when close in energy, some states are strongly localized in real space, while others spread over a larger number of spin configurations. This reflects quite naturally on a large relative variance. While the growth of $\mathcal{R}_{P_S}(t > t_{\mathrm{R}})$ with $L$ in the intermediate region ($h = 2$) seems to be exponential, in the localized phase ($h = 4$), it is linear.

## C.  Intermediate Times: $\mathbf{\Gamma^{-1} < t < t_R}$

At intermediate times, $\Gamma^{-1} < t < t_R$, one sees that the oscillations that show in the evolution of $\langle P_S(t) \rangle$ are reflected also in oscillations for $\mathcal{R}_{P_S}(t)$. The envelope of the oscillations of $\langle P_S(t) \rangle$ follow a power-law decay [63, 64]. In the chaotic region, the power-law behavior is mostly caused by the presence of the edges of the spectrum [63, 64], where the eigenstates are not chaotic. Beyond chaos, the power-law decay is caused by correlations between the components of the eigenstates [60, 61]. The lack of chaotic states in both scenarios justifies the values of $\mathcal{R}_{P_S}(t)$ above 1 seen for times $t \sim 10J^{-1}$.

Another interesting feature appears after these oscillations and before saturation. When the eigenvalues have some level of correlation, be it in the chaotic regime or in the intermediate region between chaos and localization, $\langle P_S(t) \rangle$ shows a dip below the saturation point $\langle \overline{P_S} \rangle$, which is known as correlation hole [24]. In Figs. 1 (a), (c), and (e), the dip is clearly seen below the horizontal dashed line that marks $\langle \overline{P_S} \rangle$. For reasons explained in Ref. [65], we call the time to reach the minimum of the correlation hole, Thouless time and denote it by $t_{\mathrm{Th}}$. The hole becomes less deep [66] and $t_{\mathrm{Th}}$ is postponed to longer times [65] as $h$ increases and the correlations between the eigenvalues die off [cf. Figs. 1 (a), (c), and (e)]. In the chaotic regime, there is no difference in the behavior of $\mathcal{R}_{P_S}(t)$ during or after the correlation hole [cf. Fig. 1 (a) and Fig. 1 (b)]. However, in the intermediate regime, such as for $h = 1.5$, the behavior of $\mathcal{R}_{P_S}(t)$ for $t \sim t_{\mathrm{Th}}$ and for $t > t_R$ are distinct [cf. Figs. 1 (e) and Figs. 1 (f)]. In the region of the hole, $\mathcal{R}_{P_S}(t)$ is pushed to its largest values, while for $t > t_R$, $\mathcal{R}_{P_S}(t)$ saturates at a lower point.

## IV.  INVERSE PARTICIPATION RATIO

When the system is chaotic, the inverse participation ratio is non-self-averaging at short times, but it is self-averaging at long times [29]. We show below that close to the localized phase, IPR($t$) becomes non-self-averaging at any time scale.

At short times, the evolved state $|\Psi(t)\rangle$ is not yet very far from $|\Psi(0)\rangle$, so the inverse participation ratio behaves similarly to the square of the survival probability, being therefore non-self-averaging. As shown on the right panels of Fig. 2 and in accordance with Eq. (14), $\mathcal{R}_{\mathrm{IPR}}(t)$ increases with $L$ in an equivalent way for any of the disorder strengths considered.
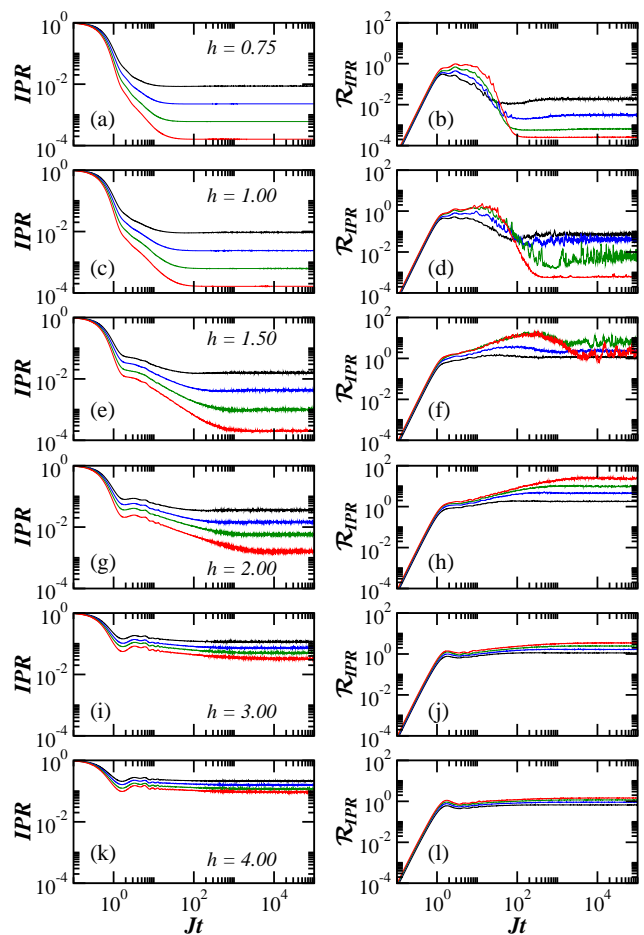


FIG. 2. Left panels: Mean value of the inverse participation ratio. Right panels: Relative variance of the inverse participation ratio. The values of the disorder are indicated on the left panels, they increase from the top to the bottom panel. The curves correspond to system sizes $L = 10$ (black), 12 (blue), 14 (green), 16 (red).

To study $\mathcal{R}_{\mathrm{IPR}}(t > t_R)$ at long times, we write the inverse participation ratio in terms of the energy eigen-

states,

$$\text{IPR}(t) = \sum_n \sum_{\alpha,\beta,\gamma,\delta} e^{-i(E_\alpha - E_\beta + E_\gamma - E_\delta)t}$$
$$\times \ c_\alpha^0 c_\alpha^{n*} c_\beta^n c_\beta^{0*} c_\gamma^0 c_\gamma^{n*} c_\delta^n c_\delta^{0*}, \qquad (20)$$

and use the same reasoning employed in the analysis of $\mathcal{R}_{P_S}(t > t_R)$. The difference now is that one has an additional sum over all unperturbed many-body states $|n\rangle$. In the chaotic regime, this significantly reduces the fluctuations leading to "super" strong self-averaging, that is, the relative variance of IPR$(t)$ decreases exponentially with $L$, as $\mathcal{R}_{\text{IPR}}(t > t_R) \propto 1/D$ [29]. We then have that before the correlation hole, $\mathcal{R}_{\text{IPR}}(t)$ increases with $L$, but later the curves for different system sizes cross and $\mathcal{R}_{\text{IPR}}(t)$ decreases with $D$ [see Fig. 2 (b)].

The picture above changes as $h$ increases from 0.75 to 1.5 and the minimum of the correlation hole moves to longer times. The crossings between the curves for $\mathcal{R}_{\text{IPR}}(t)$ happen at later times [cf. Fig. 2 (b), (d), and (f)]. Beyond these values of the disorder strength, for $h > 1.5$, the curves for the system sizes considered here no longer cross and the inverse participation ratio becomes non-self-averaging at any time scale. Just as in the case of the survival probability, for a given system size, $\mathcal{R}_{\text{IPR}}(t)$ reaches its largest values in the transition region between chaos and localization, *e.g.* for $h = 2$ in Fig. 2 (h).

Based on the results for $P_S(t)$ and IPR$(t)$, one may infer that global quantities are nowhere self-averaging in the region of fractal eigenstates and in the localized phase. Needless to say the statement awaits a proof.

## V. SPIN AUTOCORRELATION FUNCTION

The behavior of the spin autocorrelation function is just the opposite of the inverse participation ratio. $I(t)$ is always self-averaging at short times, while at long times, the dependence of $\mathcal{R}_I(t > t_R)$ on the system size is attached to the disorder strength. In the chaotic regime, just as the survival probability and contrary to the inverse participation ratio, the spin autocorrelation function is not self-averaging for $t > t_R$. As the disorder strength increases, the non-self-averaging region is pushed to ever longer times, until the system reaches the localized phase, where $I(t)$ becomes self-averaging at any time scale.

Quantities that are local in space, such as the spin autocorrelation function, are always self-averaging at short times. This holds for any value of the disorder strength and can be understood as follows. For $t < \Gamma^{-1}$, the excitations only have time to hop to few neighboring sites, even if the system is deep in the chaotic phase. As a result, due to the spatial averages given by the sum in $k$ in Eq. (12), the relative variance decreases with system size. This can be seen by expanding the relative variance
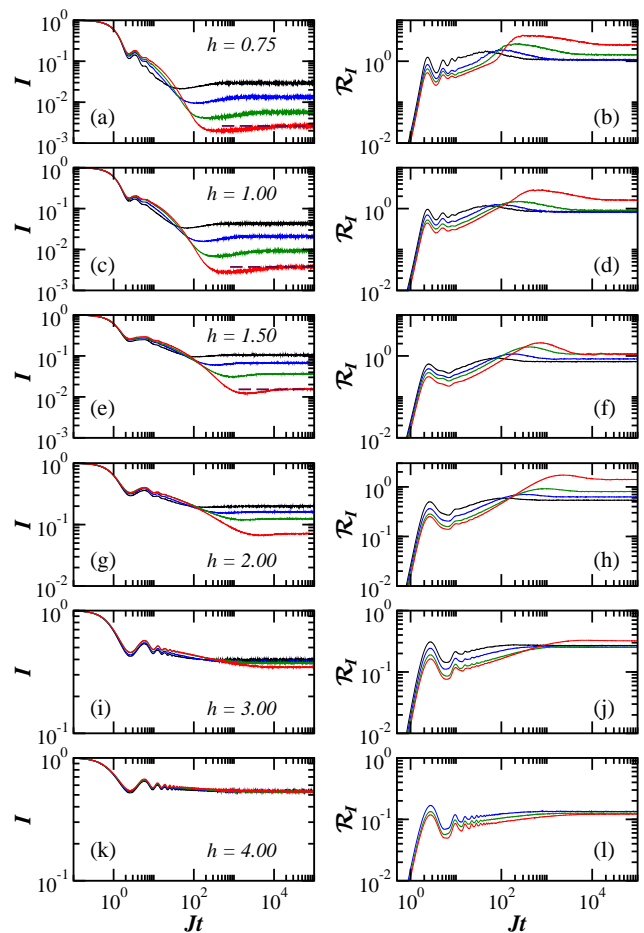


FIG. 3. Left panels: Mean value of the spin autocorrelation function. Right panels: Relative variance of the spin autocorrelation function. The values of the disorder are indicated on the left panels, they increase from the top to the bottom panel. The curves correspond to system sizes $L = 10$ (black), 12 (blue), 14 (green), 16 (red).

of the spin autocorrelation function for short times [29],

$$\mathcal{R}_I(t) = \frac{16\sigma_{\Gamma^2}^2 t^4}{L^2} + \mathcal{O}(t^6) \propto \frac{J^4 t^4}{L}. \qquad (21)$$

This result is independent of $h$, because as said in the presentation of Eq. (14), $\sigma_{\Gamma^2}$ does not depend on the disorder strength. This statement is confirmed by the right columns of Fig. 3, where the short-time behavior of $\mathcal{R}_I(t < \Gamma^{-1})$ is pretty much the same from Fig. 3 (b) to Fig. 3 (l).

Since both $P_S(t)$ and $I(t)$ are autocorrelation functions, they share important features. $I(t)$ also detects the correlation hole, as seen in Figs. 3 (a), (c), and (e), and it also keeps memory of the initial state, causing the lack of self-averaging in the chaotic and intermediate regimes at large times, as evident in Figs. 3 (b), (d), and (f).

As $h$ increases from 0.75 to 3, we should expect the crossings between the curves of $\mathcal{R}_I(t)$ to happen later

in time, analogously to what one sees in the analysis of the inverse participation ratio. This is indeed the case, but what is not yet very clear to us is why the crossings for $\mathcal{R}_I(t)$ do not happen close to $t \sim t_{\text{Th}}$, as one verifies for $\mathcal{R}_{\text{IPR}}(t)$ in Figs. 2 (b), (d), and (f). It is only for $h > 2$ that we finally see a clear shift in the crossing points of $\mathcal{R}_I(t)$ to later times. It may be that the spin autocorrelation function is more sensitive to finite size effects, but this point remains to be better understood.

In the localized phase, $h = 4$, the spin autocorrelation function finally becomes self-averaging also at very long times, as seen in Fig. 2 (l). This is because at localization, the initial spin configuration cannot change much in time. Indeed, as shown in Fig. 2 (k), the value of $I(t > t_R)$ no longer depends on the system size and saturates at a finite value. In contrast, the variance $\sigma_I^2(t)$ can still decrease with $L$, resulting in the self-averaging behavior of $I(t)$.

## VI. CONNECTED SPIN-SPIN CORRELATION FUNCTION

The connected spin-spin correlation function combines all the good properties for self-averaging found in the previous quantities. It is local, as the spin autocorrelation function, so it is self-averaging at short times for any disorder strength. Since it is not an autocorrelation function, it can be self-averaging at long times also in the chaotic regime. The result is a quantity that is self-averaging at any time scale and for any disorder strength, which is the perfect picture for an experimental quantity.

In Fig. 4, we show the absolute value of the mean value of $C(t)$ on the left columns and the relative variance on the right columns, confirming its self-averaging behavior for all $h$'s and all times. But some additional comments are in place:

(i) Despite being self-averaging everywhere, the values of the relative variance depend on the time scale and on the disorder strength. $\mathcal{R}_C(t)$ has a non-monotonic behavior in time in the chaotic and intermediate regimes, showing a dip at $t \sim 1$ and a bump at $t \sim t_{\text{Th}}$. These features are no longer seen in the localized phase [Fig. 4 (l)].

(ii) Similarly to the other three quantities, the time where the value of $\mathcal{R}_C(t)$ saturates gets postponed as the disorder strength increases [cf. Figs. 4 (b), (d), (f), (h)], happening close to the point for the minimum of the correlation hole at $t \sim t_{\text{Th}}$.

As a wrap-up, it is worth emphasizing that in the chaotic regime, all four quantities considered in this work go to zero at long times as the system size increases, yet only the survival probability and the spin autocorrelation function are non-self-averaging after saturation, while $\mathcal{R}_{\text{IPR}}(t > t_R)$ and $\mathcal{R}_C(t > t_R)$ do decrease with $L$. The fact that the denominator of $\mathcal{R}_O(t)$ goes to zero is therefore not the reason why a quantity is non-self-averaging in the chaotic regime.
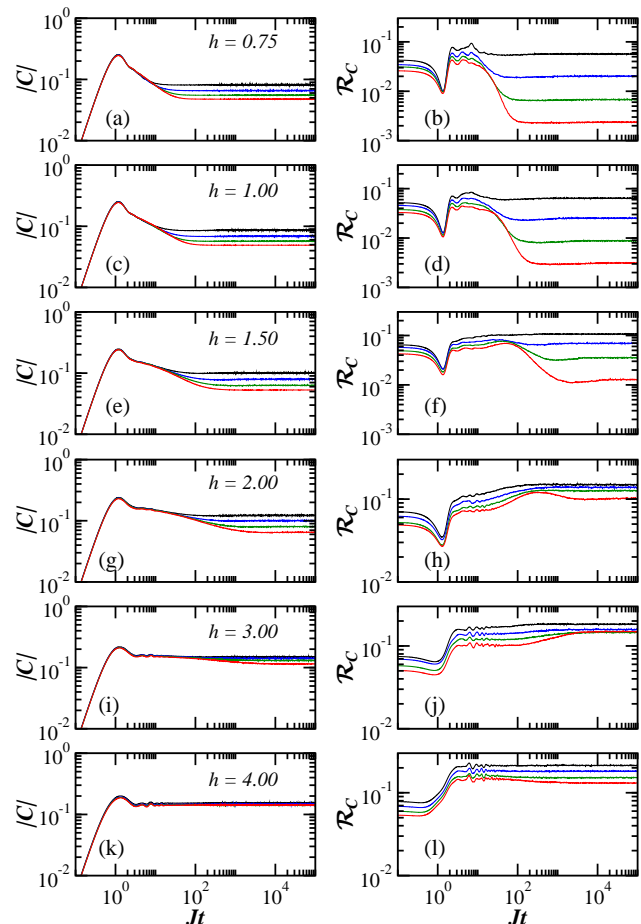


FIG. 4. Left panels: Absolute value of the mean value of the connected spin-spin autocorrelation function. Right panels: Relative variance of the connected spin-spin autocorrelation function. The values of the disorder are indicated on the left panels, they increase from the top to the bottom panel. The curves correspond to system sizes $L = 10$ (black), 12 (blue), 14 (green), 16 (red).

In the case of global quantities in localized phase, on the other hand, the combination of eigenstates of different structures, leading to reasonable values of $\sigma_O^2(t > t_R)$, together with mean values that decrease with $L$ [see Fig. 1 (k) and Fig. 2 (k)] can indeed justify their lack of self-averaging. This contrasts with the mean values of the local quantities, which do not depend on system size at long times, as shown in Fig. 3 (k) and Fig. 4 (k), resulting in their self-averaging behavior.

## VII. CONCLUSIONS

Based on the analysis of the one-dimensional spin-1/2 Heisenberg model with onsite disorder, this work shows that the self-averaging behavior of many-body quantum systems out of equilibrium is rather non-trivial, depending on the quantity, time scale, and disorder strength.

The general picture that we draw for the four quantities studied here is the following.

• The survival probability, which is non-local in real space and non-local in time, is non-self-averaging at any time scale and for any disorder strength.

• The connected spin-spin correlation function measured in experiments with ion traps, which is local in space and in time, is self-averaging at all times and for any disorder strength.

• In between these two extremes, we find the inverse participation ratio, which is non-local in space and local in time, and the spin autocorrelation function, which is local in space and non-local in time. They show complementary behaviors. In the chaotic regime, IPR$(t)$ is non-self-averaging at short times, but it becomes self-averaging at long times, while for $I(t)$, we have just the opposite. As the disorder strength increases, the crossing point between one behavior and the other gets delayed to longer times. Once localization is reached, the inverse participation ratio, just as the survival probability becomes nowhere self-averaging, while the spin autocorrelation function, just as the spin-spin correlation function, becomes self-averaging at all times.

The lack of self-averaging behavior of the survival probability is worrisome, since this quantity is extensively considered in studies of non-equilibrium quantum dynamics and in fundamental questions of quantum mechanics, such as the quantum speed limit. In fact, this quantity is now even analyzed experimentally [67]. On the positive side, among the different features that $\mathcal{R}_{P_S}(t)$ presents at different times, we single out one that is particularly useful. After saturation, as explained in Sec. III, $\mathcal{R}_{P_S}(t > t_{\mathrm{R}}) \simeq 1$ in the chaotic regime. Away from chaos, $\mathcal{R}_{P_S}(t > t_{\mathrm{R}})$ reaches values larger than 1, the largest values for a fixed system size, happening when the eigenstates become fractal. This may serve as a good diagnosis of the presence of fractality.

Contrary to ergodicity and thermalization, self-averaging in many-body quantum systems out of equilibrium has received very little attention. There are still plenty of questions that can be addressed, from extensions to other isolated time-independent Hamiltonians, to time-dependent Hamiltonians and open systems. Our own current interest is in the distributions of the expectation values of different observables at different time scales.

[1] I. M. Lifshitz, S. A. Gredeskul, and L. A. Pastur, *Introduction to the Theory of Disordered Systems* (Wiley, New York, 1988).

[2] S. Wiseman and E. Domany, *Lack of self-averaging in critical disordered systems*, Phys. Rev. E **52**, 3469 (1995).

[3] A. Aharony and A. B. Harris, *Absence of self-averaging and universal fluctuations in random systems near critical points*, Phys. Rev. Lett. **77**, 3700 (1996).

[4] S. Wiseman and E. Domany, *finite-size scaling and lack of self-averaging in critical disordered systems*, Phys. Rev. Lett. **81**, 22 (1998).

[5] T. Castellani and A. Cavagna, *Spin-glass theory for pedestrians*, J. Stat. Mech. Th. Exp. **2005**, P05012 (2005).

[6] A. Malakis and N. G. Fytas, *Lack of self-averaging of the specific heat in the three-dimensional random-field Ising model*, Phys. Rev. E **73**, 016109 (2006).

[7] S. Roy and S. M. Bhattacharjee, *Is small-world network disordered?*, Phys. Lett. A **352**, 13 (2006).

[8] C. Monthus, *Random Walks and Polymers in the Presence of Quenched Disorder*, Lett. Math. Phys. **78**, 207 (2006).

[9] A. Efrat and M. Schwartz, *Lack of self-averaging in random systems - Liability or asset?*, Phys. A Stat. Mech. Appl. **414**, 137 (2014).

[10] M. Łobejko, J. Dajka, and J. Łuczka, *Self-averaging of random quantum dynamics*, Phys. Rev. A **98**, 022111 (2018).

[11] J.-P. Bouchaud and A. Georges, *Anomalous diffusion in disordered media: Statistical mechanisms, models and physical applications*, Phys. Rep. **195**, 127 (1990).

[12] T. Akimoto, E. Barkai, and K. Saito, *Universal Fluctuations of Single-Particle Diffusivity in a Quenched Environment*, Phys. Rev. Lett. **117**, 180602 (2016).

[13] A. Russian, M. Dentz, and P. Gouze, *Self-averaging and weak ergodicity breaking of diffusion in heterogeneous media*, Phys. Rev. E **96**, 022156 (2017).

[14] T. Akimoto, E. Barkai, and K. Saito, *Non-self-averaging behaviors and ergodicity in quenched trap models with finite system sizes*, Phys. Rev. E **97**, 052143 (2018).

[15] L. Pastur and M. V. Shcherbina, *Absence of self-averaging of the order parameter in the Sherrington-*

*Kirkpatrick model*, J. Stat. Phys. **62**, 1 (1990).

[16] W. Wreszinski and O. Bolina, *A self-averaging "order parameter" for the Sherrington-Kirkpatrick spin glass model*, J. Stat. Phys. **116**, 1389 (2004).

[17] G. Parisi and N. Sourlas, *Scale invariance in disordered systems: The example of the random-field Ising model*, Phys. Rev. Lett. **89**, 257204 (2002).

[18] C. A. Müller and D. Delande, *Disorder and interference: localization phenomena*, les Houches 2009 - Session XCI: Ultracold Gases and Quantum Information, C. Miniatura, L.-C. Kwek, M. Ducloy, B. Gremaud, B.-G. Englert, L.F. Cugliandolo, A. Ekert, eds. (Oxford University Press, Oxford 2011); arXiv:1004.0915.

[19] L. Pastur and V. Slavin, *Area Law Scaling for the Entropy of Disordered Quasifree Fermions*, Phys. Rev. Lett. **113**, 150404 (2014).

[20] O. S. Barišić, J. Kokalj, I. Balog, and P. Prelovšek, *Dynamical conductivity and its fluctuations along the crossover to many-body localization*, Phys. Rev. B **94**, 045126 (2016).

[21] P. Prelovšek, M. Mierzejewski, O. Barišić, and J. Herbrych, *Density correlations and transport in models of many-body localization*, Ann. Phys. (Berlin) **529**, 1600362 (2017).

[22] M. Serbyn, Z. Papić, and D. A. Abanin, *Thouless energy and multifractality across the many-body localization transition*, Phys. Rev. B **96**, 104201 (2017).

[23] B. Mukherjee, *Floquet topological transition by unpolarized light*, Phys. Rev. B **98**, 235112 (2018).

[24] L. Leviandier, M. Lombardi, R. Jost, and J. P. Pique, *Fourier transform: A tool to measure statistical level properties in very complex spectra*, Phys. Rev. Lett. **56**, 2449 (1986).

[25] N. Argaman, F.-M. Dittes, E. Doron, J. P. Keating, A. Y. Kitaev, M. Sieber, and U. Smilansky, *Correlations in the actions of periodic orbits derived from quantum chaos*, Phys. Rev. Lett. **71**, 4326 (1993).

[26] B. Eckhardt and J. Main, *Semiclassical Form Factor of Matrix Element Fluctuations*, Phys. Rev. Lett. **75**, 2300 (1995).

[27] R. E. Prange, *The spectral form factor is not self-averaging*, Phys. Rev. Lett. **78**, 2280 (1997).

[28] P. Braun and F. Haake, *Self-averaging characteristics of spectral fluctuations*, J.Phys. A **48**, 135101 (2015).

[29] M. Schiulaz, E. J. Torres-Herrera, F. Pérez-Bernal, and L. F. Santos, *Self-averaging in many-body quantum systems out of equilibrium*, arXiv:1906.11856.

[30] M. Schreiber, S. S. Hodgman, P. Bordia, H. P. Lüschen, M. H. Fischer, R. Vosk, E. Altman, U. Schneider, and I. Bloch, *Observation of many-body localization of interacting fermions in a quasirandom optical lattice*, Science **349**, 842 (2015).

[31] P. Richerme, Z.-X. Gong, A. Lee, C. Senko, J. Smith, M. Foss-Feig, S. Michalakis, A. V. Gorshkov, and C. Monroe, *Non-local propagation of correlations in quantum systems with long-range interactions*, Nature **511**, 198 (2014).

[32] M. Srednicki, *Thermal fluctuations in quantized chaotic systems*, J. Phys. A **29**, L75 (1996).

[33] P. Reimann, *Foundation of statistical mechanics under experimentally realistic conditions*, Phys. Rev. Lett. **101**, 190403 (2008).

[34] A. J. Short, *Equilibration of quantum systems and subsystems*, New J. Phys. **13**, 053009 (2011).

[35] P. R. Zangara, A. D. Dente, E. J. Torres-Herrera, H. M. Pastawski, A. Iucci, and L. F. Santos, *Time fluctuations in isolated quantum systems of interacting particles*, Phys. Rev. E **88**, 032913 (2013).

[36] L. F. Santos, G. Rigolin, and C. O. Escobar, *Entanglement versus chaos in disordered spin systems*, Phys. Rev. A **69**, 042304 (2004).

[37] F. Dukesz, M. Zilbergerts, and L. F. Santos, *Interplay between interaction and (un)correlated disorder in one-dimensional many-particle systems: delocalization and global entanglement*, New J. Phys. **11**, 043026 (2009).

[38] A. Pal and D. A. Huse, *Many-body localization phase transition*, Phys. Rev. B **82**, 174411 (2010).

[39] R. Nandkishore and D. Huse, *Many-body localization and thermalization in quantum statistical mechanics*, Annu. Rev. Condens. Matter Phys. **6**, 15 (2015).

[40] D. Luitz and Y. B. Lev, *The ergodic side of the many-body localization transition*, Ann. Phys.(Berlin) **529**, 1600350 (2017).

[41] L. A. Khalfin, *Contribution to the decay theory of a quasi-stationary state*, Sov. Phys. JETP **6**, 1053 (1958).

[42] L. Fonda, G. C. Ghirardi, and A. Rimini, *Decay theory of unstable quantum systems*, Rep. Prog. Phys. **41**, 587 (1978).

[43] K. Bhattacharyya, *Quantum decay and the Mandelstam-Tamm-energy inequality*, J. Phys. A **16**, 2993 (1983).

[44] R. Ketzmerick, G. Petschel, and T. Geisel, *Slow decay of temporal correlations in quantum systems with Cantor spectra*, Phys. Rev. Lett. **69**, 695 (1992).

[45] J. G. Muga, A. Ruschhaupt, and A. del Campo, *Time in Quantum Mechanics, vol. 2* (Springer, London, 2009).

[46] E. J. Torres-Herrera and L. F. Santos, *Quench dynamics of isolated many-body quantum systems*, Phys. Rev. A **89**, 043620 (2014).

[47] E. J. Torres-Herrera, M. Vyas, and L. F. Santos, *General features of the relaxation dynamics of interacting quantum systems*, New J. Phys. **16**, 063010 (2014).

[48] E. J. Torres-Herrera and L. F. Santos, *Local quenches with global effects in interacting quantum systems*, Phys. Rev. E **89**, 062110 (2014).

[49] E. J. Torres-Herrera and L. F. Santos, *Nonexponential fidelity decay in isolated interacting quantum systems*, Phys. Rev. A **90**, 033623 (2014).

[50] P. P. Mazza, J.-M. Stéphan, E. Canovi, V. Alba, M. Brockmann, and M. Haque, *Overlap distributions for quantum quenches in the anisotropic Heisenberg chain*, J. Stat. Mech. **2016**, 013104 (2016).

[51] E. J. Torres-Herrera, A. M. García-García, and L. F. Santos, *Generic dynamical features of quenched interacting quantum systems: Survival probability, density imbalance, and out-of-time-ordered correlator*, Phys. Rev. B **97**, 060303 (2018).

[52] A. Volya and V. Zelevinsky, *Time-dependent relaxation of observables in complex quantum systems*, arXiv:1905.11918.

[53] S. Bera, G. De Tomasi, I. M. Khaymovich, and A. Scardicchio, *Return probability for the Anderson model on the random regular graph*, Phys. Rev. B **98**, 134205 (2018).

[54] S. Lerma-Hernández, J. Chávez-Carlos, M. A. Bastarrachea-Magnani, L. F. Santos, and J. G. Hirsch, *Analytical description of the survival probability of coherent states in regular regimes*, J. Phys. A **51**, 475302 (2018).

[55] P. Reimann, *Typical fast thermalization processes in closed many-body systems*, Nat. Comm. **7**, 10821 (2016).

[56] P. Reimann, *Transportless equilibration in isolated many-body quantum systems*, New J. Phys. **21**, 053014 (2019).

[57] F. Borgonovi, F. M. Izrailev, and L. F. Santos, *Exponentially fast dynamics of chaotic many-body systems*, Phys. Rev. E **99**, 010101 (2019).

[58] F. Borgonovi, F. M. Izrailev, and L. F. Santos, *Timescales in the quench dynamics of many-body quantum systems: Participation ratio versus out-of-time ordered correlator*, Phys. Rev. E **99**, 052143 (2019).

[59] A. De Luca, B. L. Altshuler, V. E. Kravtsov, and A. Scardicchio, *Anderson localization on the Bethe lattice: Nonergodicity of extended states*, Phys. Rev. Lett. **113**, 046806 (2014).

[60] E. J. Torres-Herrera and L. F. Santos, *Dynamics at the many-body localization transition*, Phys. Rev. B **92**, 014208 (2015).

[61] E. J. Torres-Herrera and L. F. Santos, *Extended nonergodic states in disordered many-body quantum systems*, Ann. Phys. (Berlin) **529**, 1600284 (2017).

[62] M. Pino, V. E. Kravtsov, B. L. Altshuler, and L. B. Ioffe, *Multifractal metal in a disordered josephson junctions array*, Phys. Rev. B **96**, 214205 (2017).

[63] M. Távora, E. J. Torres-Herrera, and L. F. Santos, *Inevitable power-law behavior of isolated many-body quantum systems and how it anticipates thermalization*, Phys. Rev. A **94**, 041603 (2016).

[64] M. Távora, E. J. Torres-Herrera, and L. F. Santos, *Power-law decay exponents: A dynamical criterion for predicting thermalization*, Phys. Rev. A **95**, 013604 (2017).

[65] M. Schiulaz, E. J. Torres-Herrera, and L. F. Santos, *Thouless and relaxation time scales in many-body quantum systems*, Phys. Rev. B **99**, 174313 (2019).

[66] E. J. Torres-Herrera and L. F. Santos, *Dynamical manifestations of quantum chaos: correlation hole and bulge*, Philos. Trans. Royal Soc. A **375**, 20160434 (2017).

[67] K. Singh, C. J. Fujiwara, Z. A. Geiger, E. Q. Simmons, M. Lipatov, A. Cao, P. Dotti, S. V. Rajagopal, R. Senaratne, T. Shimasaki, et al., *Quantifying and controlling prethermal nonergodicity in interacting Floquet matter*, arXiv:1809.05554.